bioRxiv preprint doi: https://doi.org/10.1101/2021.08.06.455469; this version posted August 8, 2021. The copyright holder for this preprint (which was not certified by peer review) is the author/funder. All rights reserved. No reuse allowed without permission.

Recombinant NAGLU-IGF2 prevents physical and neurological disease and improves survival in Sanfilippo B syndrome

Steven Q. Le,[1*] Shih-hsin Kan,[2*] Marie Nuñez,[3] Joshua Dearborn,[3] Feng Wang,[4] Shan Li,[4] Liz Snella,[5] Jackie K. Jens,[5] Bethann N. Valentine,[5] Hemanth R. Nelvagal,[1] Alexander Sorensen,[1] Jonathan D. Cooper,[1] Tsui-Fen Chou,[4] N. Matthew Ellinwood,[5] Jodi D. Smith,[6] Mark S. Sands,[3] and Patricia I. Dickson[1**]

1. Department of Pediatrics, Washington University School of Medicine, St. Louis, Missouri, USA

2. CHOC Research Institute, Orange, California, USA

3. Department of Medicine, Washington University School of Medicine, St. Louis, Missouri, USA

4. Department of Biology and Biological Engineering, California Institute of Technology, Pasadena, California, USA

5. Department of Animal Science, Iowa State University, Ames, Iowa, USA

6. Department of Veterinary Pathology, Iowa State University, Ames, Iowa, USA

*co-first authors

**Correspondence to:

Patricia I. Dickson, MD

4444 Forest Park Ave, Ste 5400

St. Louis, MO 63108

(314) 273-2943

pdickson@wustl.edu

bioRxiv preprint doi: https://doi.org/10.1101/2021.08.06.455469; this version posted August 8, 2021. The copyright holder for this preprint (which was not certified by peer review) is the author/funder. All rights reserved. No reuse allowed without permission.

Abstract

Recombinant human alpha-*N*-acetylglucosaminidase-insulin-like growth factor-2 (rhNAGLU-IGF2) is an investigational enzyme replacement therapy for Sanfilippo B, a lysosomal storage disease. The fusion protein with IGF2 permits binding to the cation-independent mannose 6-phosphate receptor, because recombinant human NAGLU (rhNAGLU) is poorly mannose 6-phosphorylated. We previously administered rhNAGLU-IGF2 intracerebroventricularly to Sanfilippo B mice. We demonstrated therapeutic restoration of NAGLU, normalization of lysosomal storage, and improvement in markers of neurodegeneration and inflammation. Here, we studied intracerebroventricular rhNAGLU-IGF2 in murine and canine Sanfilippo B to determine potential effects on the behavioral phenotype and survival. Heparan sulfate (HS) levels in brain and heart were reduced following treatment with rhNAGLU-IGF2 or rhNAGLU. Treated mice showed improvement in disease markers such as beta-hexosaminidase, CD68, and LAMP1. We found a more normal number of stretch attend postures, a fear pose, in mice treated with either rhNAGLU or rhNAGLU-IGF2 vs vehicle-treated Sanfilippo B mice on elevated plus maze testing ($p<0.001$). We found a more normal dark/light activity pattern in Sanfilippo B mice treated with rhNAGLU-IGF2 compared to vehicle-treated Sanfilippo B mice ($p=0.025$). We found a 61% increase in survival in Sanfilippo B mice treated with rhNAGLU-IGF2 (mean 53d, median 48d) compared to vehicle-treated Sanfilippo B mice (mean 33d, median 37d; $p<0.001$). In canine Sanfilippo B, we found that rhNAGLU-IGF2 administered into cerebrospinal fluid normalized heparan sulfate and beta-hexosaminidase activity in gray and white matter brain regions. Proteomics analysis of cerebral cortex showed restoration of protein concentrations in pathways relevant to cognitive function, synapse, and the lysosome. Treatment with rhNAGLU-IGF2 may improve the phenotype of Sanfilippo B disease.

Keywords: mucopolysaccharidosis, enzyme replacement therapy, glycosaminoglycan, proteomics, lysosomal storage disease

bioRxiv preprint doi: https://doi.org/10.1101/2021.08.06.455469; this version posted August 8, 2021. The copyright holder for this preprint (which was not certified by peer review) is the author/funder. All rights reserved. No reuse allowed without permission.

Introduction

Lysosomal storage diseases are a heterogenous group of inherited disorders characterized by accumulation of some substrate within lysosomes. Generally, these are caused by an inability to perform an enzymatic reaction, often due to deficiency in the production or function of a lysosomal hydrolase. In the clinic, some of these soluble lysosomal hydrolases are available in recombinant form and may be delivered by repeated infusion into the bloodstream or into the cerebrospinal fluid[1–7].

To function as a therapeutic enzyme, a recombinant lysosomal hydrolase requires proper post-translational modification including glycosylation with mannose 6-phosphate.[8] Mannose 6-phosphate residues bind to mannose 6-phosphate receptors expressed on the endosomal-lysosomal membrane, which transports the enzyme from the Golgi apparatus to the lysosome, where it is active and catabolizes substrate in the acidic environment of that compartment. One of the lysosomal hydrolases, the enzyme alpha-*N*-acetyl-glucosaminidase (NAGLU) that is responsible for Sanfilippo B syndrome (or mucopolysaccharidosis type IIIB, MPS IIIB), is not properly processed when produced recombinantly.[9,10] A fusion protein that contains the therapeutic enzyme (recombinant human alpha-*N*-acetyl-glucosaminidase; rhNAGLU) plus a peptide fragment consisting of the M6PR binding region of IGF2 (forming rhNAGLU-IGF2) demonstrated improved intracellular uptake and reduction of lysosomal storage in Sanfilippo B fibroblasts.[11] Using a mouse model, we administered rhNAGLU-IGF2 intracerebroventricularly, demonstrating therapeutic restoration of NAGLU, normalization of lysosomal storage, and dramatic improvement in markers of neurodegeneration and inflammation.[12] Neonatally administered rhNAGLU-IGF2 showed an effect duration of more than four weeks after a single ICV dose.[13] A commercial form of rhNAGLU-IGF2 has reached clinical trials.[14–16]

Sanfilippo (types A-D) is together one of the most common lysosomal storage diseases, with incidence estimates ranging from 1/100,000 to 1/25,000.[17,18] Approximately fifteen percent of Sanfilippo disease is type B. [17] The lysosomal storage material in Sanfilippo syndromes is the glycosaminoglycan heparan sulfate. The disease is associated with progressive neurodegeneration, typically with onset in early childhood.[18]

Recombinant enzymes delivered into cerebrospinal fluid can penetrate into deep brain structures and improve neuropathology in preclinical studies,[19–22] and there is one recombinant therapeutic enzyme approved for intracerebroventricular administration in patients for the late-infantile form of neuronal ceroid lipofuscinosis (CLN2 disease).[6] Here, we studied the effect of intracerebroventricular rhNAGLU-IGF2 on behavior and survival in Sanfilippo B mice and studied biochemical effects and proteomics in the brain of neonatal Sanfilippo B dogs.

bioRxiv preprint doi: https://doi.org/10.1101/2021.08.06.455469; this version posted August 8, 2021. The copyright holder for this preprint (which was not certified by peer review) is the author/funder. All rights reserved. No reuse allowed without permission.

Methods

Mouse model: *Naglu*-/- mice (B6.129S6-*Naglu*$^{tm1Efn/J}$, backbred onto the C57BL6/J strain for at least 10 generations) were produced by crossing -/- male mice with +/- female mice, thus generating approximately ½ affected. Mice received research forms of recombinant human NAGLU-IGF2 (100 µg), NAGLU (100 µg), or an equivalent volume (~5 µl) of vehicle at 28-day intervals via the left lateral ventricle beginning at PND 2. At four weeks of age, mice were cannulated into the left ventricle and doses infused over 5 minutes (1µl/min). Research forms of NAGLU-IGF2, NAGLU, and vehicle were provided by Biomarin Pharmaceutical, Inc. Experimental personnel were blinded as to treatment or vehicle (coded "1, 2 or 3"). Cannulated mice were housed with carrier female companions. All animal experiments were approved by the institutional animal use committees.

Behavior: Male Sanfilippo B "mutant" mice and male heterozygous "carrier" mice were used for the behavior assessment at the UCLA Behavior Core. Mice of both sexes were used for studies at Washington University School of Medicine in St. Louis. Mice received rhNAGLU, rhNAGLU-IGF2, or vehicle at four week intervals beginning at post-natal day 2.

Elevated plus maze, novel object recognition, and social interaction tests were performed at the UCLA Behavioral Testing Core as previously described.[23] The final infusion dose was given at 16 weeks of age, then the cannulae were removed before behavior testing at 16-20 weeks of age was performed. Mice in these experiments were male and cannulae prevented them from being caged with other males. To prevent confounding of behavioral experiments due to social isolation, these males were cohoused with a female companion and permitted to breed.

To test balance (vestibular and cerebellar function), cohorts of mice of mixed gender were studied at Washington University School of Medicine in St. Louis, Missouri. Animals were tested on UGO Basile, rota-rod at 32 and 40 weeks as described.[24] Briefly, a rocking paradigm with reversal of direction of rotation after each full turn at 10 rpm for 3 minutes was executed for 3 consecutive days at 32 and 40 weeks of age. For each time point, entrainment was done for 2 consecutive days with 3 trials each day and 20 minutes of rest between each trial. Testing occurred on the third consecutive day and the length of time each mouse remained on the rod was recorded for all three trials and averaged. Activity in an open field was assessed over 24 h in a rectangular polystyrene enclosure surrounded by photobeams monitored by computer software (MotorMonitor, Kinder Scientific, Poway, CA).[25] Testing consisted first of a 12 h block with the room lights off ("dark") and eded with a 12 h block with the room lights on ("light"). Mice had access to food and water ad libitum during testing. Outcome measures included rearings, distance traveled, and time spent resting. The mice were sacrificed at 40 weeks old following behavioral assessments.

Survival: In the survival experiment mutant mice were given monthly infusion starting at PND2 with vehicle (8 males, 8 females) or rhNAGLU-IGF2 (8 males, 8 females) as well as carrier mice given vehicle (3 males, 13 females) or rhNAGLU-IGF2 (8 males, 8 females). The survival experiment was carried to humane endpoints and terminated with the death of the last treated mutant mice.

Biochemical assays: NAGLU activity and total hexosaminidase activity were quantified using 4-methylumbelliferyl assays as previously described.[12] Briefly the catalytic activity of NAGLU and of NAGLU–IGFII was determined by hydrolysis of the fluorogenic substrate, 4-

bioRxiv preprint doi: https://doi.org/10.1101/2021.08.06.455469; this version posted August 8, 2021. The copyright holder for this preprint (which was not certified by peer review) is the author/funder. All rights reserved. No reuse allowed without permission.

methylumbelliferyl-*N*-acetyl-α-glucosaminide, obtained from CalBiochem (now EMD Millipore Chemicals) or Toronto Research Chemicals, with minor modifications of a published protocol, using 1.0 mM substrate in the incubation mixture.[26] Catalytic activity of β-hexosaminidase (combined A and B isoforms) was determined by hydrolysis of 4-methylumbelliferyl-*N*-acetyl-β-glucosaminide (EMD Millipore Chemicals) using 1.25 mM substrate in the incubation mixture. For both enzymes, a unit of activity is defined as release of 1 nmol of 4-methylumbelliferone (4MU) per hour. Protein concentration was estimated by the Bradford method, using bovine serum albumin as a standard.

Analysis of heparan sulfate was performed by Biomarin Pharmaceutical (mouse tissues) or the UC San Diego GlycoAnalytics Core (canine tissues) as described previously.[27] Tissues were homogenized and digested overnight with Pronase (Sigma-Aldrich) in phosphate-buffered at 37 °C and centrifuged at 14 000 rpm for 20 min. The supernatant was passed through a DEAE column, and the bound GAG was eluted with 2 M NaCl. The GAG was then desalted on PD10-size exclusion column, and purified GAG was lyophilized. Dried GAG disaccharides were dissolved in aniline and reacted with freshly prepared sodium cyanoborohydride solution in a dimethyl sulfoxide/acetic acid mixture (7:3, v/v). Reactions were carried out at 65 °C for 1 h followed by 37 °C for 16 h. The samples were then dried using a speed vacuum at room temperature and used for further analysis by glycan reductive isotope labeling (GRIL) LTQ-MS. Aniline-tagged disaccharides were separated on a C18 column using an ion pairing solvent mixture and analyzed by mass spectrometry in negative ion mode.

Immunostaining: Mice were anesthetized with isoflurane and perfused transcardially with heparinized PBS followed by 4% formaldehyde in neutral PBS. After post-fixation in this solution for an additional 48 hours, the brains were removed and cryoprotected in 30% sucrose in 50 mM tris buffered saline. A one in six series of 40 µm coronal brain sections from each mouse were stained on slides using a modified immunofluorescence protocol for the following antibodies: rat anti-mouse CD68, 1:400, Bio-Rad, rabbit anti-LAMP1, 1:400, abcam, rabbit anti-ATP synthase C (SCMAS), 1:400, abcam. The intensity of immunostaining was assessed using a semi-automated thresholding image analysis method, as described previously, using Image Pro-Premier software (MediaCybernetics, Chicago, IL).[28] Brain areas included the striatum, somatosensory cortex, and entorhinal cortex.

Canine model: Canine experiments were conducted at Iowa State University under protocols approved by the institutional animal care and use committee. Sanfilippo B dogs were produced by breeding homozygous affected males to carrier females. Affected dogs were anesthetized and a 22 gauge needle inserted into the cisterna magna as described. CSF (0.2 to 0.5 ml) was collected freeflowing. A syringe was attached to the needle hub to deliver rhNAGLU-IGF2 (diluted to 3 ml in sterile saline) over 2-3 minutes. Dose was calculated per estimated brain weight. At one week of age, canine brains are roughly 1/38 of body weight, and the administered dose was 400 mg rhNAGLU-IGF/kg brain, or approximately 7 mg. For a 2.5 kg four week-old pup, in which brain weight is 1/60 of body weight, the dose was approximately 17 mg. Dogs in the treatment group received rhNAGLU-IGF2 at 1 week of age and again at 4 weeks of age and were euthanized at 8 weeks of age (4 weeks after the second dose). Control group animals were not treated. At necropsy, terminal CSF and blood were collected, and dogs were perfused with chilled PBS and brains removed. Brains were sliced coronally into 4 mm slabs using a pre-chilled, stainless steel canine brain matrix (ASI Instruments) as described elsewhere.[29] A 3 mm

bioRxiv preprint doi: https://doi.org/10.1101/2021.08.06.455469; this version posted August 8, 2021. The copyright holder for this preprint (which was not certified by peer review) is the author/funder. All rights reserved. No reuse allowed without permission.

skin punch was used to collect samples from cerebral gray matter, cerebral white matter, caudate, and cerebellar vermis. Samples were snap-frozen in an isopentane bath on dry ice.

Proteomics Using tissue slabs that had been frozen on isopentane and dry ice and stored at -80 °C, we dissected samples (approximately 1x1x0.4 cm) from a parasagittal gyrus, including gray matter and subcortical white matter. Canine brain samples were analyzed for 2,814 proteins by LC/MS/MS at the laboratory of Tsui-Fen Chou (Caltech). 100 µg of canine brain cortex samples were prepared for mass spectrometry acquisition using Thermo EasyPep Mini MS Sample Prep Kit (cat# A4006). After determing peptide concentrations by Pierce Quantitative Fluorometric Peptide Assay (cat# 23290), 20 µg peptide from each sample was labeled with TMT10plex Isobaric Label Reagent Set (Thermo, cat# A37725) following to the manufacture's instruction. Labeled samples were combined and dried using vacuum centrifugation. Samples were then separated into 8 fractions using the High pH reversed-phase peptide Fractionation Kit (Thermo, cat# 84868). The fractions were dissolved with 0.1% FA and peptide concentration was determined with Quantitative Colorimetric Peptide Assay (Thermo, cat# 23275).

TMT labeling LC-MS/MS experiments were performed using an EASY-nLC 1000 connected to an Orbitrap Eclipse Tribrid mass spectrometer. 0.5 µg of each fraction was loaded onto an Aurora UHPLC Column and separated over 131 min at a flow rate of 0.4 µL/min with the following gradient: 2-6% Solvent B (2 min), 6-22% B (78 min), 22-50% B (40 min), 50-95% B (1 min), and 95% B (10 min). Solvent A consisted of 97.8% H_2O, 2% ACN, and 0.2% formic acid, and solvent B consisted of 19.8% H_2O, 80% ACN, and 0.2% formic acid. An MS1 scan was acquired in the Orbitrap at 120k resolution with a scan range of 400-1600 m/z. The AGC target was 1×10^6, and the maximum injection time was 50 ms. Dynamic exclusion was set to exclude features after 1 time for 60 s with a 10-ppm mass tolerance. MS2 scans were acquired with CID activation type with the IonTrap. The isolation window was 0.7 m/z, the collision energy was 35%, the maximum injection time was 35 ms and the AGC target was 1×10^4. MS3 scans were acquired with HCD activation type in the Orbitrap at 60k resolution with a scan range of 100-500 m/z. The isolation window was 0.7 m/z, the collision energy was 65%, the maximum injection time was 118 ms and the AGC target was 2.5×10^5. Ion source settings were as follows: ion source type, NSI; spray voltage, 2300 V; ion transfer tube temperature, 300°C. System control and data collection were performed by Xcalibur software.

Data analysis: Graphs were produced on GraphPad Prism or SigmaPlot version 14.0 (Systat). Linear regression was performed using SigmaPlot. Statistical analysis of continuous variables was performed on Stata (version 16) using ANOVA. The proteomic data processing was performed through Proteome Discoverer 2.4 (Thermo) using Uniprot canine database and the SequestHT with Percolator validation. Normalization was performed relative to the total peptide amount. Further analyses were performed as below: limma analyses were performed using R studio following the user guide;[30] volcano plot was generated with Origin 2019b; DE proteins were tested for enrichment analysis using g:Profiler[31] and plotted with Prism 7; heatmaps were generated with Prism 7.

bioRxiv preprint doi: https://doi.org/10.1101/2021.08.06.455469; this version posted August 8, 2021. The copyright holder for this preprint (which was not certified by peer review) is the author/funder. All rights reserved. No reuse allowed without permission.

Results

Lysosomal storage: Male and female mice received rhNAGLU-IGF2, rhNAGLU, or vehicle at PND2. They were cannulated at 4 weeks of age and received rhNAGLU-IGF2 or vehicle at 4 week intervals until 16 weeks and sacrificed at 20 weeks. Brain and heart showed a reduction in HS that reached statistical significance for each treatment group compared to vehicle-treated MUT mice ($p<0.001$, **Fig. 1**). All intergroup differences were statistically significant by unadjusted ANOVA. There was some residual NAGLU enzymatic activity detected in mouse brains in both treatement groups despite the 28-day interval from the final dose and tissue collection (**Supplemental Table S1**). We found improvement in disease markers such as beta-hexosaminidase (**Supplemental Table S2**), CD68 (**Fig. 2**), and LAMP1 (**Fig. 3**) in mice treated with rhNAGLU or rhNAGLU-IGF2.

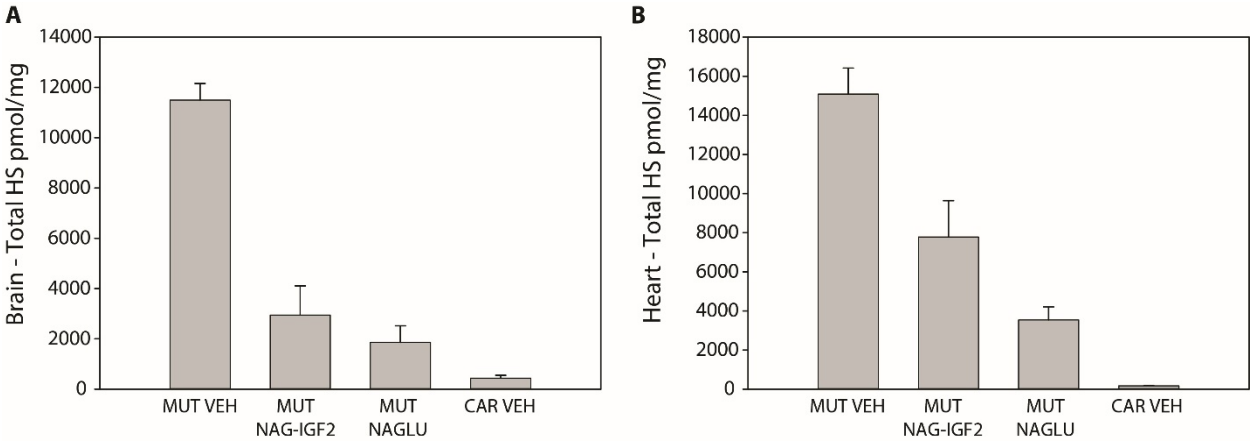

Fig. 1. Heparan sulfate (HS) concentrations in the brain and heart of experimental mice and controls. MUT: Sanfilippo B (*Naglu-/-*) mice. CAR: heterozygous carrier (*Naglu +/-*) mice that are expected to be phenotypically unaffected. VEH: vehicle. NAG-IGF2: recombinant human NAGLU-IGF2, NAGLU: recombinant human NAGLU. Treatments and vehicle were administered intracerebroventricularly as described in the methods. N=8 per group.

bioRxiv preprint doi: https://doi.org/10.1101/2021.08.06.455469; this version posted August 8, 2021. The copyright holder for this preprint (which was not certified by peer review) is the author/funder. All rights reserved. No reuse allowed without permission.

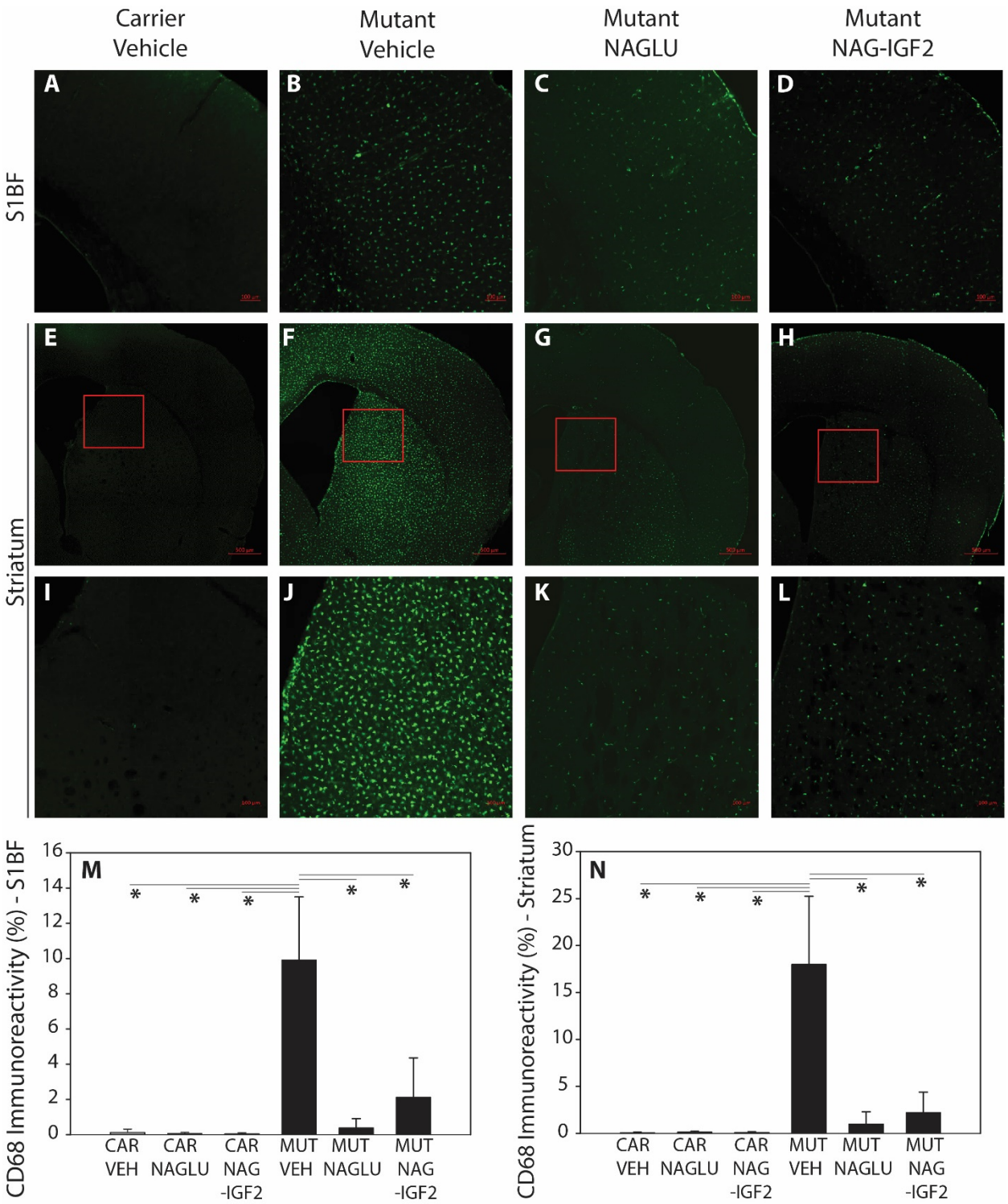

Fig. 2. Immunofluorescence staining with anti-CD68 (green) in the primary somatosensory cortex (S1BF) and striatum (caudate and putamen) in mice. Red boxes indicate insets for the panels below. Bar graphs depict means and standard deviations of thresholding image analysis. N=4-9 per group. *p<0.01.

bioRxiv preprint doi: https://doi.org/10.1101/2021.08.06.455469; this version posted August 8, 2021. The copyright holder for this preprint (which was not certified by peer review) is the author/funder. All rights reserved. No reuse allowed without permission.

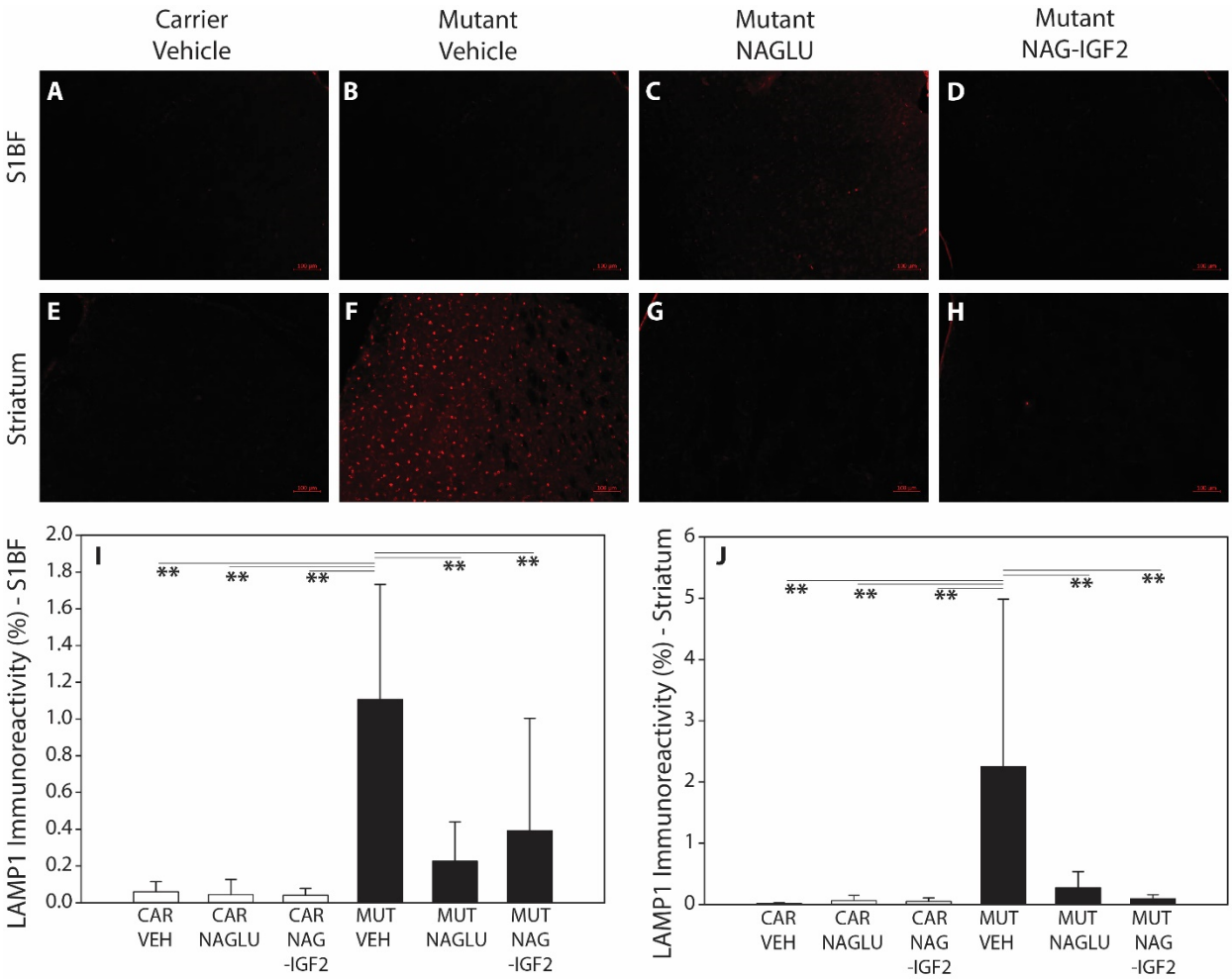

Fig. 3. Immunofluorescence staining with anti-LAMP1 (red) in the primary somatosensory cortex (S1BF) and striatum (caudate and putamen) in mice. Bar graphs depict means and standard deviations of thresholding image analysis. N=4-9 per group. **p<0.001.

Behavior: Male Sanfilippo B and control mice were treated with rhNAGLU, rhNAGLU-IGF2, or vehicle from PND2 to 16 weeks as described in the methods. We previously found that Sanfilippo B mice show reduced fear, as evidenced by decreased stretch attend postures on the elevated plus maze.[23] This intergroup difference was again seen here (**Fig. 4**), with a more normal number of stretch attend postures in mice treated with either rhNAGLU or rhNAGLU-IGF2.

bioRxiv preprint doi: https://doi.org/10.1101/2021.08.06.455469; this version posted August 8, 2021. The copyright holder for this preprint (which was not certified by peer review) is the author/funder. All rights reserved. No reuse allowed without permission.

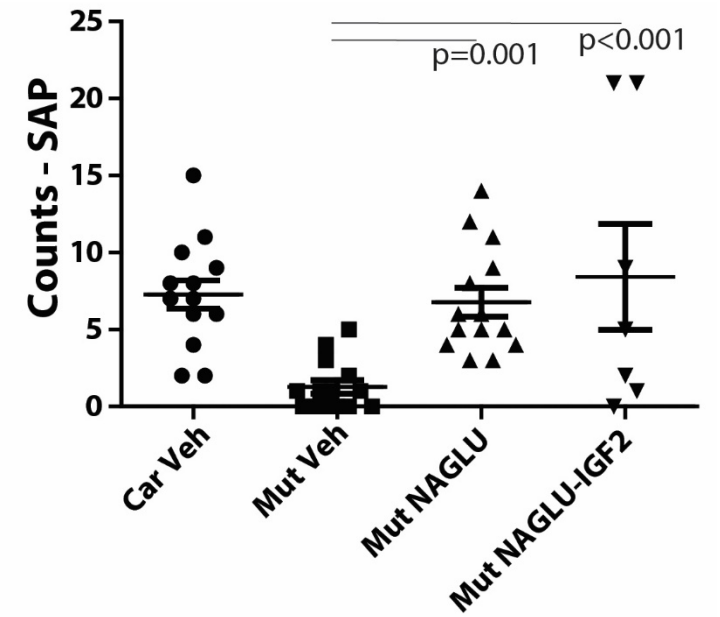

Fig. 4 Count of stretch attend postures during testing on the elevated plus maze. Carrier ("Car") mice are *Naglu*+/-, mutant ("Mut") are *Naglu*-/-. Carrier and mutant mice were treated with vehicle ("Veh"). Carrier mice treated with rhNAGLU or rhNAGLU-IGF2 did not differ from carrier mice treated with vehicle (not shown). Each dot = one mouse, with means and s.e.m. shown. N=7-16 per group.

We did not find significant intergroup differences between vehicle-treated Sanfilippo B mice and controls in radial arm maze, social interaction testing, and novel object recognition testing (**Supplemental Figures S1-S4**).

Survival: Sanfilippo B and control mice were treated with rhNAGLU-IGF2 or vehicle (four groups; **Fig. 5**). The experiment was terminated after the last mutant mouse died. Results indicate a 58% increase in survival in Sanfilippo B mice treated with rhNAGLU-IGF2 (mean 52d, median 48d) compared to vehicle-treated Sanfilippo B mice (mean 33d, median 37d; $p<0.001$). Causes of death and other adverse events (mainly loss of cannulae and reimplantation) are described in **Supplemental Table S3**.

bioRxiv preprint doi: https://doi.org/10.1101/2021.08.06.455469; this version posted August 8, 2021. The copyright holder for this preprint (which was not certified by peer review) is the author/funder. All rights reserved. No reuse allowed without permission.

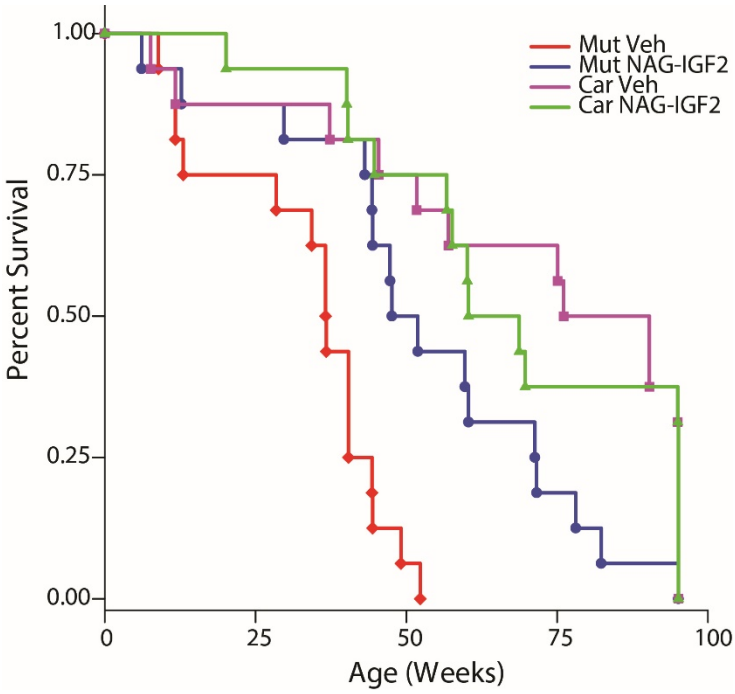

Fig. 5. Survival curves for Sanfilippo B mice (Mut) and carrier controls (Car) treated with ICV vehicle (Veh) or rhNAGLU-IGF2 (NAG-IGF2) monthly from PND 2. N=16 per group, males and females. P<0.001 Mut-Veh v Mut-NAG-IGF2.

Dark/light activity: Patients with Sanfilippo B show abnormal circadian rhythm, including poor or inverted sleep patterns.[32] Sanfilippo B mice and controls were treated from PND 2 with monthly rhNAGLU-IGF2 or vehicle (four groups). At age 22 weeks, Sanfilippo B mice showed greater activity during the dark phase than heterozygous control mice (**Fig. 6**). A more normal sleep/activity pattern was seen in Sanfilippo B mice treated with rhNAGLU-IGF2. Total rest was similar across groups, but vehicle-treated Sanfilippo B mice covered more total distance than treated mutant mice or carrier controls, although this difference did not reach statistical significance.

bioRxiv preprint doi: https://doi.org/10.1101/2021.08.06.455469; this version posted August 8, 2021. The copyright holder for this preprint (which was not certified by peer review) is the author/funder. All rights reserved. No reuse allowed without permission.

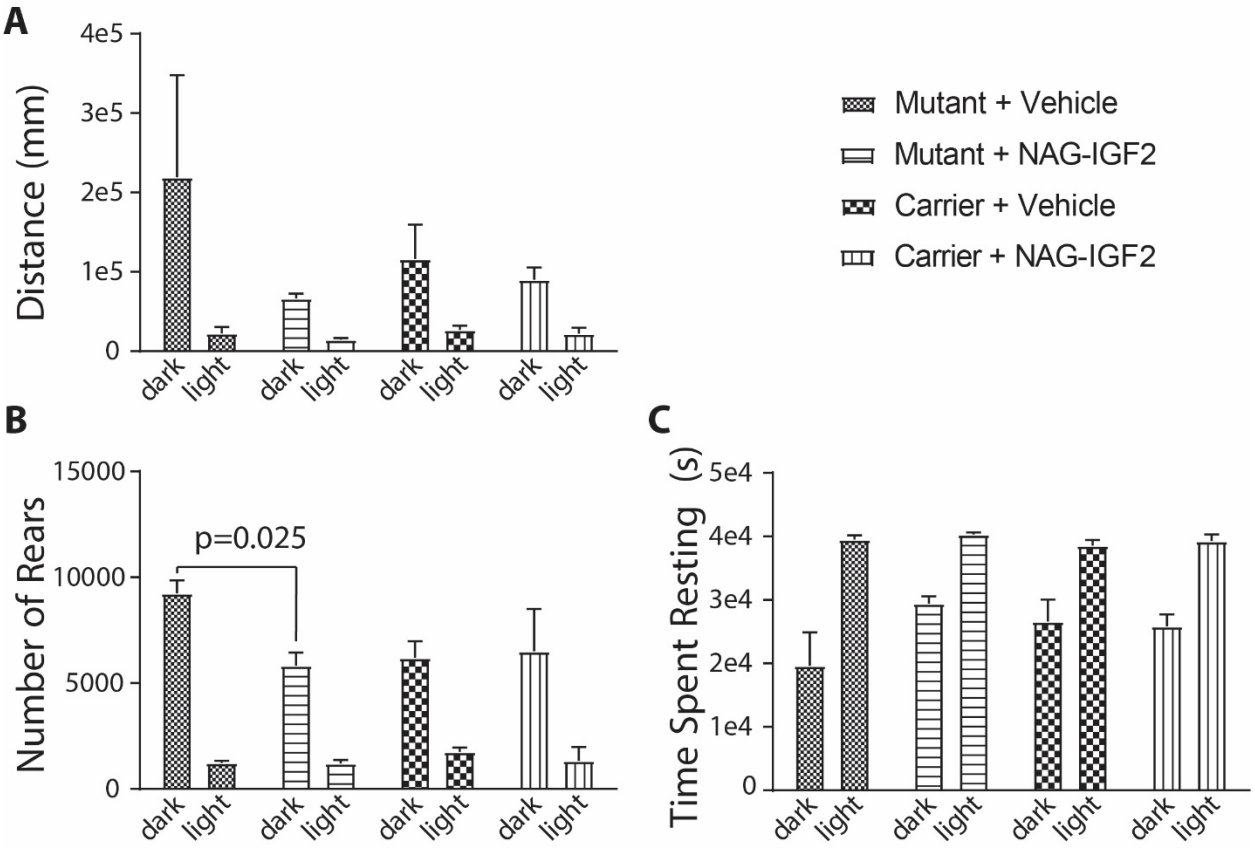

Fig. 6 Activity in dark and light phases of open field by genotype and treatment group. Mutant + vehicle, n=3. Mutant + NAG-IGF2, n=9. Carrier + vehicle, n=20. Carrier + NAG-IGF2, n=3.

Motor Coordination: This experiment involves Sanfilippo B mice and controls treated from PND 2 with monthly rhNAGLU-IGF2 or vehicle (4 groups). Rotarod testing at 32 and 40 weeks are shown in **Fig. 7**. Sanfilippo B mice treated with vehicle (Mut - Vehicle; n=3) showed slightly reduced rotarod performance at 32 weeks ($p<0.001$), with further worsening at 40 weeks ($p<0.001$). Sanfilippo B mice treated with rhNAGLU-IGF2 (Mut – NAG-IGF2, n=9) showed no reduction in rotarod performance at 32 weeks, but showed a decrease in performance at 40 weeks compared to vehicle-treated or rhNAGLU-IGF2-treated carrier mice, but remained significantly better than vehicle-treated mutant mice (all $p<0.001$). One Sanfilippo B mouse treated with vehicle died between weeks 32 and 40.

bioRxiv preprint doi: https://doi.org/10.1101/2021.08.06.455469; this version posted August 8, 2021. The copyright holder for this preprint (which was not certified by peer review) is the author/funder. All rights reserved. No reuse allowed without permission.

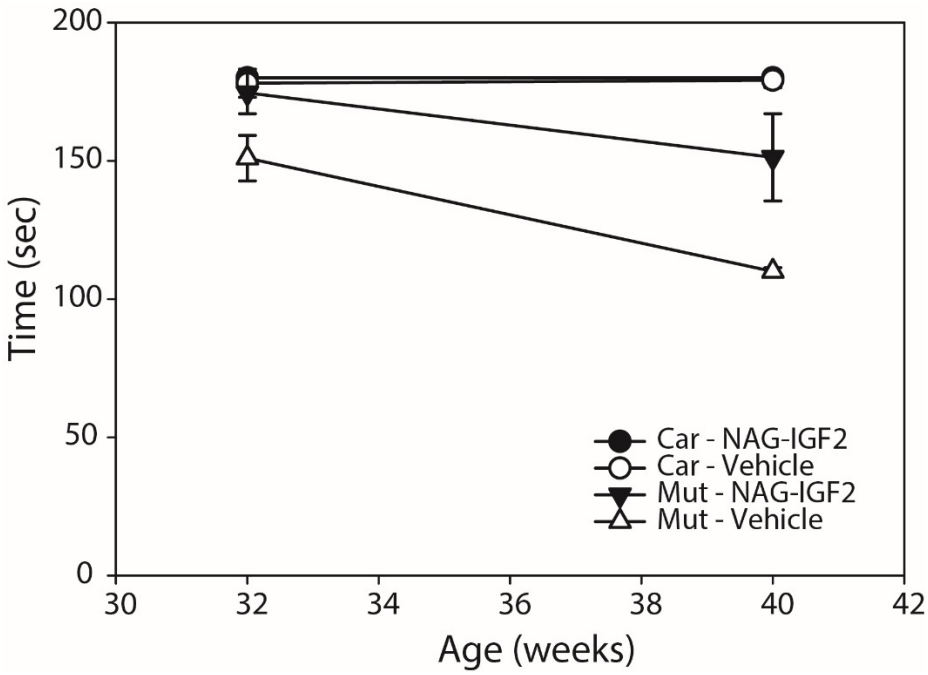

Fig. 7 Time to fall off rotarod in Carrier (+/-) and Mut (-/-) Sanfilippo B mice treated with vehicle or NAGLU-IGFII (NAG-IGF2) ICV monthly from PND 2. Mice were studied at 32 and 40 weeks. P<0.001 for MUT-Vehicle v MUT-NAG-IGF2 at both timepoints.

Canine studies: In this experiment, three Sanfilippo B dogs received two doses of rhNAGLU-IGF2, approximately 7 mg at 1 week and approximately 17 mg at 4 weeks of age, into the cerebrospinal fluid at the cisterna magna and were sacrificed at 8 weeks of age, four weeks following the second and final dose. Three untreated Sanfillipo B dogs and three untreated carrier dogs were used as controls. Sanfilippo B dogs showed increased HS and beta-hexosaminidase levels in most brain regions compared to controls (**Fig. 8**). These were reduced essentially to normal levels in treated animals, even in deeper regions of brain such as white matter and caudate nucleus. Some NAGLU activity was detected in brain tissue despite a four-week interval from the date of the final rhNAGLU-IGF2 dose and tissue collection (**Supplemental Table S4**).

bioRxiv preprint doi: https://doi.org/10.1101/2021.08.06.455469; this version posted August 8, 2021. The copyright holder for this preprint (which was not certified by peer review) is the author/funder. All rights reserved. No reuse allowed without permission.

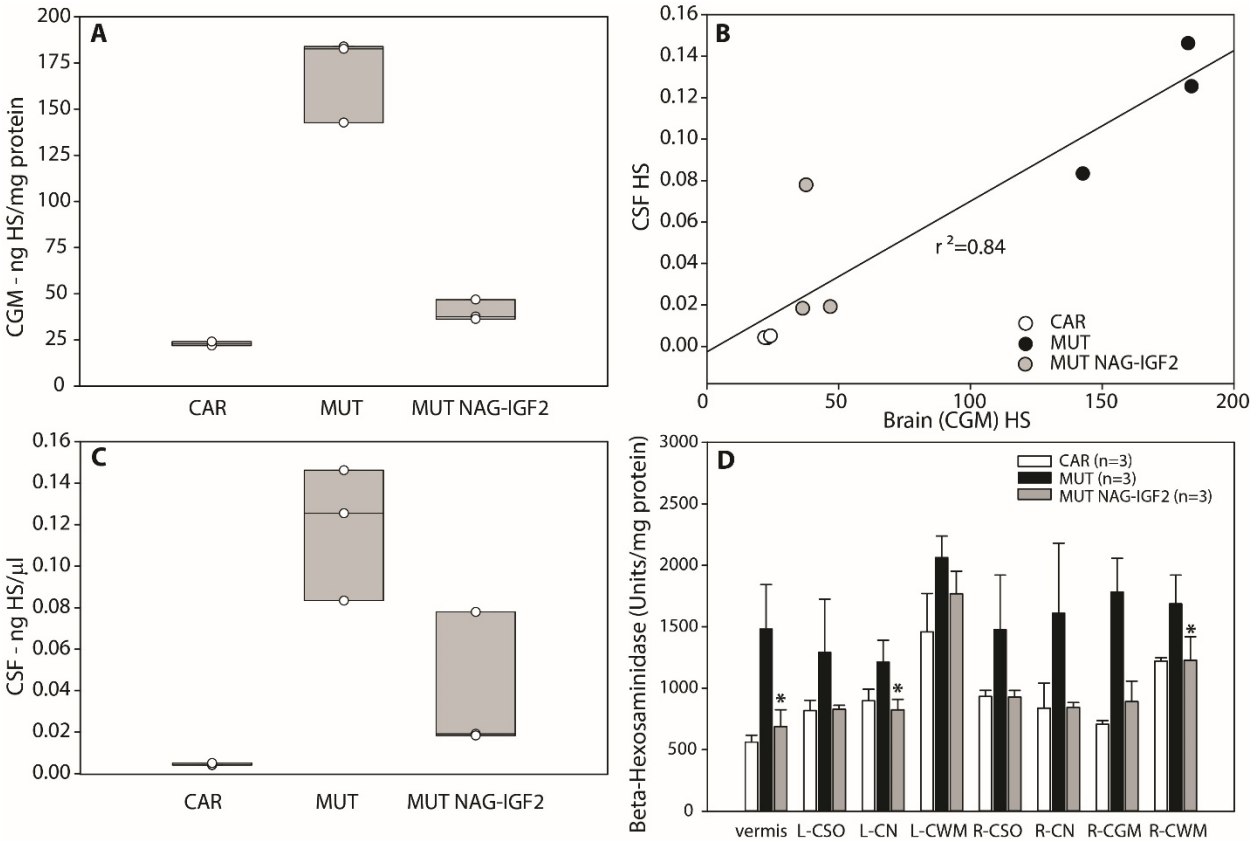

Fig. 8 Sanfilippo B dogs (MUT) and carrier controls (CAR) were treated with intra-cisternal rhNAGLU-IGF2 (NAG-IGF2) or untreated at 1 and 4 weeks of age and sacrificed at 8 weeks (n=3 per group, both sexes). (A) Box plot of heparan sulfate (HS) in left cerebral gray matter (CGM). Open circles represent individual animals. MUT v CAR and MUT NAG-IGF2 v CAR were statistically significant at $p<0.01$. (B) Regression curve showing HS in cerebrospinal fluid (CSF) versus HS in CGM. (C) Box plot of heparan sulfate (HS) in CSF. Open circles represent individual animals. MUT v CAR and MUT NAG-IGF2 v CAR were statistically significant at $p<0.01$. (D) Beta-hexosaminidase in brain regions (means and standard deviation). CSO: centrum semiovale. CN: caudate nucleus. CGM: cerebral gray matter. CWM: cerebral white matter. *$p<0.05$ NAG-IGF2 v MUT.

Proteomics was performed on cerebral cortical samples of each animal at the Chou lab as described in the Methods (**Fig. 9**). Tandem mass tag (TMT) 10-plexed labelling was employed to evaluate the proteomic changes caused by Sanfilippo B mutant. Specifically, we prepared three independent biological wild type (CAR), Sanfilippo B (MUT) and rhNAGLU-IGF2-treated Sanfilippo B (ERT) canine brain cortex samples. The TMT labeled samples were pooled and further fractionated into 8 fractions, and analyzed with the RTS-SPS-MS3 method. A total of 5806 proteins were identified and of which 4442 proteins were quantified across all 9 samples (**Supplemental Table S5**). We identified 309 proteins that demonstrated significantly different quantities ($p < 0.05$) between the Sanfilippo B (MUT) and wild type (CAR) samples (**Supplemental Table S6**) by limma analysis. Among them, a set of 41 proteins with $\log_2$(fold

bioRxiv preprint doi: https://doi.org/10.1101/2021.08.06.455469; this version posted August 8, 2021. The copyright holder for this preprint (which was not certified by peer review) is the author/funder. All rights reserved. No reuse allowed without permission.

change) >0.5 (up-regulated) or <-0.5 (down-regulated) was classified as the final differentially expressed proteins (DEPs) (**Fig. 9A, Supplemental Table S7**). Subsequently, functional enrichment analysis were performed on the 41 DEPs. The top four relevant changed cellular component in the significantly enriched GO terms and top four changed KEGG or REAC functional pathways are presented in **Fig. 9B**. The GO: CC analysis showed these DEPs are mainly located at lysosome, secretory granule, extracellular matrix, and vesicle. And the pathway analysis indicated the DEPs primarily related to Glycosaminoglycan degradation, Keratan sulfate degradation, Neutrophil degranulation, and Innate Immune System. Furthermore, we examined if the ERT treatment could reverse the dysregulated protein level caused by Sanfilippo B mutant. As shown in **Fig. 9C**, ERT therapy reversed several mutant caused down regulations, such as DPP7 and CALB2. Notably, most of the up regulations caused by Sanfilippo B mutant could be reversed by ERT treatment, such as GNS, LAMP1, HEXB, CD63, etc. These results provide valuable insights for identifying novel hallmarks of lysosomal diseases and therapeutic targets for the Sanfilippo B.

bioRxiv preprint doi: https://doi.org/10.1101/2021.08.06.455469; this version posted August 8, 2021. The copyright holder for this preprint (which was not certified by peer review) is the author/funder. All rights reserved. No reuse allowed without permission.

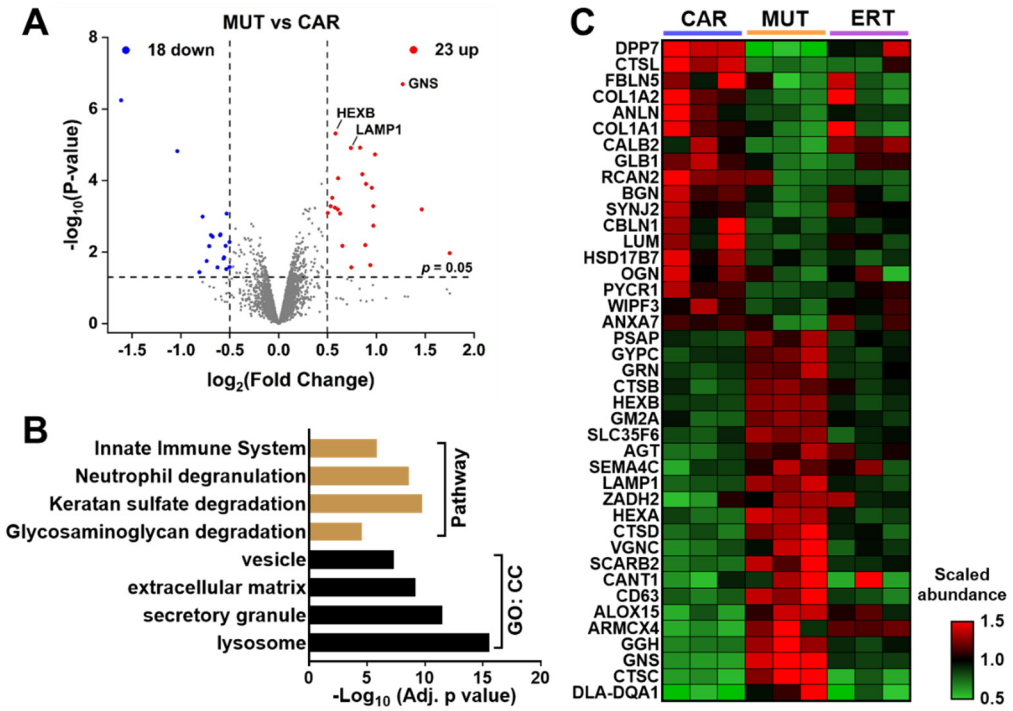

Fig. 9 Proteomic analysis of wild type (CAR), Sanfilippo B (MUT) and rhNAGLU-IGF2-treated Sanfilippo B (ERT) canine brain cortex. A) Volcano plot displaying the proteomic changes in Sanfilippo B mutant, n=3. B) Functional enrichment analysis on the DEPs affected by Sanfilippo B mutant. C) Heatmap displaying the scaled abundance of the DEPs affected by Sanfilippo B mutant and ERT treatment.

bioRxiv preprint doi: https://doi.org/10.1101/2021.08.06.455469; this version posted August 8, 2021. The copyright holder for this preprint (which was not certified by peer review) is the author/funder. All rights reserved. No reuse allowed without permission.

Discussion

Previously, we studied the biochemical and pathological efficacy of ICV rhNAGLU-IGF2 in Sanfilippo B mice. Here, we attempted to assess its effectiveness on behavior and survival. Our behavioral assessments were designed to separately evaluate the behavior that might be impacted by physical disease, such as motor activity and balance, from behavior that would be expected to be primarily representative of neocortical function, such as fear behavior. We found evidence that rhNAGLU-IGF2 improved survival, physical disease, and fear behavior in Sanfilippo B mice. Some but not all of these studies also included an experimental group that received rhNAGLU (without IGF2), and we found an equivalent improvement in the outcomes we evaluated in the rhNAGLU-treated mice as the rhNAGLU-IGF2-treated mice.

Our study had a number of important limitations. First, the rhNAGLU-IGF2 that was available for our studies was not materially the same as the clinical candidate that is currently in clinical trials. We do not know the differences in composition between the clinical candidate material and the research form that we used here. Second, our studies were not designed to evaluate the biodistribution of either rhNAGLU or rhNAGLU-IGF2 in the central nervous system. This is because our chosen study termination occurred four weeks after the final dose, following behavioral studies. The half-life of rhNAGLU-IGF2 in the brain was previously estimated at approximately seven days, although mice treated at postnatal day 1 or 2 showed NAGLU activity at four weeks following a single ICV injection of rhNAGLU-IGF2.[13] However, the dose (100 µg) was not increased as the mice grew, so that in this study little to no enzyme could be detected in the brain of these mice at four weeks after the final infusion. This limitation also meant that we were unable to determine the cellular distribution of the enzymes in tissues. Third, some behavioral assessments such as radial arm maze and social interaction test did not show intergroup differences between carriers and affected mice during this experiment, so that we could not use these tests to determine whether there was a therapeutic effect in treated cohorts. Mice were cannulated, which may have affected the behavior and clearly limited the types of experiments we could conduct; for example, we were not able to perform the Morris water maze.

Our results raise the question of the importance of mannose 6-phosphate receptor-mediated uptake in effective enzyme replacement therapy for the brain. Studies in vitro using human fibroblasts demonstrate that efficient uptake of lysosomal enzymes into this cell type is nearly completely dependent on mannose 6-phosphate receptors. Similarly, neuronal cell lines appear to also rely on mannose 6-phosphate receptors for intracellular uptake, suggesting that treating these critical cells requires the use of this system.[13,33,34] Conversely, in vitro and in vivo studies Sanfilippo B and other lysosomal disorders have demonstrated that macrophage-lineage cells do not depend entirely on mannose 6-phosphate receptors to engulf material from the extracellular milieu,[35,36] and this was observed for mouse microglial cells incubated with rhNAGLU.[33] A limited study by the Neufeld laboratory found that rhNAGLU administered intravenously to Sanfilippo B mice localized to tissue macrophages.[37] Notably, macrophage targeting was sufficient to nearly normalize heparan sulfate levels in systemic tissues that were accessible to circulating enzyme from the bloodstream. This raises two possibilities: either macrophage-targeting is sufficient to treat Sanfilippo B disease, or perhaps more likely, whole-tissue measurements of heparan sulfate do not sufficiently characterize a therapeutic response.

bioRxiv preprint doi: https://doi.org/10.1101/2021.08.06.455469; this version posted August 8, 2021. The copyright holder for this preprint (which was not certified by peer review) is the author/funder. All rights reserved. No reuse allowed without permission.

Microglia are macrophage-lineage cells of the central nervous system, and expected therefore to take up even enzymes that lack mannose 6-phosphate residues or their equivalent. There is ample evidence of microgliosis in Sanfilippo B disease,[29,38,39] but the role of microglial activation and other inflammatory cascades is not clear. One possibility in explaining our findings is that the behavioral and neuropathological outcomes that are frequently used to evaluate Sanfilippo B mice may reflect the inflammatory component of the disease. Treatment of Sanfilippo B mice with the immunosuppressive steroid prednisolone improved rotarod performance and survival, suggesting a prominent role of inflammation in the manifestations of disease in the mouse model.[40] An unanswered question, therefore, is whether this "inflammatory component" is the primary disease driver of neurological impairment in Sanfilippo B disease in both the mouse model, and more importantly, in humans.

Alternatively, another possible explanation for our findings is that the dose and frequency we chose did not reveal a difference between rhNAGLU and rhNAGLU-IGF2 that might otherwise have been apparent. We observed that neither rhNAGLU nor rhNAGLU-IGF2 completely treated Sanfilippo B disease in this experiment. It is possible that a different dose or frequency of rhNAGLU-IGF2 administration, would have demonstrated a more robust therapeutic effect compared to rhNAGLU. If the dose and frequency were too high, nonspecific uptake would be expected to occur and possibly eliminate the differences between the enzymes. Alternatively, if the dose were too low, microglial and perivascular cell uptake could have been predominant in both the rhNAGLU and rhNAGLU-IGF2-treated groups. In this scenario, both rhNAGLU and rhNAGLU-IGF2 would have treated mainly these glial cells and not sufficiently treated the neurons directly, resulting in a phenotypic improvement corresponding to correction in inflammatory and other supportive cells only. Even with enzymes that are well mannose 6-phosphorylated, such as recombinant human alpha-L-iduronidase (for Hurler syndrome also known as MPS I) for example, distribution studies of intravenously administered enzyme showed preferential localization in sinusoidal cells with lesser staining appearing in hepatocytes. There could be a "threshold effect" at work, in which saturating macrophage-lineage cells is necessary prior to sufficient uptake into the target cells. It is not clear whether rhNAGLU or rhNAGLU-IGF2 were taken up into neurons in vivo in the brain during the experiments described here, because we were not able to assess biodistribution in our studies for the reasons described above. Previously published studies of rhNAGLU-IGF2 did show staining for NAGLU in neurons,[12] but the dosing interval for that study was higher – five doses in two weeks – compared to the monthly dosing described here. If monthly dose and frequency of administration of rhNAGLU-IGF2 was inadequate to treat neurons yet sufficient to induce behavioral improvements, this implies that our phenotypic read-outs in Sanfilippo B mice are not sufficient to measure the neurological disease process and its treatment.

Besides enzyme replacement therapy, another approach in development is gene therapy to deliver the coding sequence for NAGLU as a permanent means of correction. Studies of adeno-associated viral vectors used to deliver NAGLU to Sanfilippo B mice show improvements in heparan sulfate, neuropathology, behavior, and survival that are similar to those reported here for recombinant enzyme administration.[41,42] It is not known whether cells that are transduced by viral vectors bearing the NAGLU transgene produce NAGLU that is properly mannose 6-phosphorylated. However, in vitro studies of NAGLU screted by cells transduced using adeno-associated viral vector-2 demonstrated that the secreted NAGLU was able to correct intracellular heparan sulfate accumulation as evidenced by $^{35}SO_4$ assay.[43] The authors did not study

bioRxiv preprint doi: https://doi.org/10.1101/2021.08.06.455469; this version posted August 8, 2021. The copyright holder for this preprint (which was not certified by peer review) is the author/funder. All rights reserved. No reuse allowed without permission.

competitive inhibition of this effect by mannose 6-phosphate, so it is not clear whether the enzyme used that receptor system for uptake. It has long been understood for mucopolysaccharidosis that the concentration of enzyme that is required for correction of glycaominoglycan accumulation is far lower than that required to demonstrate intracellular uptake of active enzyme.[44] To that point, both rhNAGLU-IGFII and rhNAGLU were capable of reducing intracellular heparan sulfate in human Sanfilippo B fibroblasts in vitro, although 10-fold higher concentrations of rhNAGLU compard to rhNAGLU-IGFII were required to achieve this effect.[33] To study mannose 6-phosphorylation of NAGLU in the context of gene therapy, induced pluripotent stem cells derived from Sanfilippo B mouse embryonic fibroblasts were transduced with lentivirus bearing the human NAGLU transgene under a cytomegalovirus promoter.[45] The supernatant from these cells was added to NAGLU human fibroblasts in the presence or absence of mannose 6-phosphate. The study demonstrated uptake of NAGLU from the supernatant of these lentiviral-modified cells into Sanfilippo B fibroblasts that was nearly completely abolished with the addition of mannose 6-phosphate to the media, suggesting that NAGLU produced by gene therapy may not suffer the same post-translational processing issues as NAGLU produced by recombinant (plasmid) methods.

The importance of treating systemic disease due to Sanfilippo B syndrome is also not known. Cardiac involvement is described in patients, including valvular heart disease, myocardial thickening, and arrhythmia.[46,47] The course is progressive, and while currently cardiac involvement is not a driver of mortality or even major symptoms due to Sanfilippo B syndrome, it seems probable that if neurological disease is treated the morbidity from heart disease would be more evident. Cerebrospinal fluid bulk turnover occurs multiple times per day (approximately three times per day in humans), and so it is expected that recombinant enzymes administered into the cerebrospinal fluid would reach the blood circulatory system, from which they would be taken up by organs and tissues outside the central nervous system. It is not known whether this approach of delivering enzymes to the cerebrospinal fluid in order to treat both the central nervous system and the rest of the body, would be sufficient, holistic therapy for Sanfilippo disease.

Canine proteomics results showed alterations in lysosomal proteins, such as elevation of alpha-N-acetylglucosamine-6-sulfatase (GNS), cathepsin D (CTSD), and beta-hexosaminidase (HEXB). These results are not surprising, as lysosomal enzymes and other proteins may show elevated activity levels in tissues of Sanfilippo B mice compared to controls. Marked deficiency in the protein dipeptidyl peptidase 7 (DPP7), has not to our knowledge been previously associated with Sanfilippo B syndrome. Dipeptidyl peptidase 7 is a serine protease that localizes to non-lysosomal vesicles and shows substrate specificity similar to that of the cell-surface protein dipeptidyl peptidase 4.[48] Interestingly, HS and heparin oligosaccharides may inhibit the activity of dipeptidyl peptidase 4.[49] Low expression of collagen type I alpha1 (COL1A1), collagen type I alpha2 (COL1A2), and fibulin 5 (FBLN5), proteins implicated in connective tissue disorders, was found in Sanfilippo dogs compared to controls, with more normal expression in treated animals. Deficiency in collagen and fibulin is not known to be associated with Sanfilippo syndrome, although these proteins and HS-containing proteoglycans are components of the extracellular matrix.

Conclusions:

bioRxiv preprint doi: https://doi.org/10.1101/2021.08.06.455469; this version posted August 8, 2021. The copyright holder for this preprint (which was not certified by peer review) is the author/funder. All rights reserved. No reuse allowed without permission.

Long-term treatment with monthly intracerebroventricular rhNAGLU-IGF2 (research form) showed a beneficial effect in Sanfilippo B mice. Significant intergroup differences were noted in survival, motor activity, stretch attend postures (fear behavior), microglial activation, and lysosomal substrate accumulation and its markers (beta-hexosaminidase, LAMP1) between enzyme-treated and vehicle-treated Sanfilippo B mice. Whole tissue brain and heart HS were lower in Sanfilippo B mice treated with rhNAGLU compared to rhNAGLU-IGF2. We did not detect other intergroup differences between rhNAGLU and rhNAGLU-IGF2-treated mice in the outcome measures that we assessed in these experiments. Notably, our studies were not designed to assess NAGLU distribution, and only one experiment included treatment groups with both enzymes. Sanfilippo B dogs treated with rhNAGLU-IGF2 showed less HS in brain and CSF compared to untreated affected controls, with beta-hexosaminidase acitivity normalized to carrier levels in most cerebral areas including gray and white matter regions. Proteomics studies in cerebral cortex showed dysregulated pathways in Sanfilippo B dogs compared to carrier controls, with restoration of a more normal pattern in Sanfilippo B dogs treated with rhNAGLU-IGF2. These findings suggest that rhNAGLU-IGF2 administered into cerebrospinal fluid shows a beneficial effect on the Sanfilippo B phenotype.

Acknowledgements:

P.I.D., J.D., M.S.S., and J.D.C. designed experiments and prepared the manuscript. S.Q.L., S.-h.K., M.N., and J.D. performed mouse experiments. S.Q.L, A.S., H.R.N., and J.D.C. performed quantitative immunofluorescence. L.S., B.N.V., N.M.E., J.J., and J.D.S. performed canine experiments. F.W., S.L, S.Q.L., and T.F.C. performed enzyme assays and/or proteomics on canine tissues. We gratefully acknowledge the assistance and support of Soila Sukipolvi, Irina Zhuravka, George Lopez, Ling Wang, Valentina Sanguez, and Catalina Guerra. Biomarin Pharmaceutical provided vehicle, rhNAGLU, and rhNAGLU-IGF2. Biomarin provided HS measurement of mouse brain and heart tissues. We gratefully acknowledge Roger Lawrence and Brett Crawford for their specific assistance with these assays.

Conflicts of Interest:

Biomarin Pharmaceutical Inc provided research materials for this study. Dr. Dickson receives research support from Genzyme and research materials from M6P Therapeutics.

Funding:

Research was supported by R01 NS088766 to P.I.D. The Washington University Animal Behavioral services are supported by the Eunice Kennedy Shriver National Institute Of Child Health & Human Development of the National Institutes of Health under Award Number P50 HD103525 to the Intellectual and Developmental Disabilities Research Center at Washington University. The content is solely the responsibility of the authors and does not necessarily represent the official views of the National Institutes of Health. The UCLA Behavioral Testing Core is supported by the UCLA Bioscience Core Funding Initiative. Immunofluorescence imaging was performed in part through the use of Washington University Center for Cellular Imaging (WUCCI) supported by Washington University School of Medicine, The Children's Discovery Institute of Washington University and St. Louis Children's Hospital (CDI-CORE-2015-505 and CDI-CORE-2019-813) and the Foundation for Barnes-Jewish Hospital (3770 and 4642).

bioRxiv preprint doi: https://doi.org/10.1101/2021.08.06.455469; this version posted August 8, 2021. The copyright holder for this preprint (which was not certified by peer review) is the author/funder. All rights reserved. No reuse allowed without permission.

References

1 Kakkis ED, Muenzer J, Tiller GE, Waber L, Belmont J, Passage M, *et al.* Enzyme-replacement therapy in mucopolysaccharisosis I. *N Engl J Med* 2001;**344**:182–8.

2 Kishnani PS, Corzo D, Nicolino M, Byrne B, Mandel H, Hwu WL, *et al.* Recombinant human acid {alpha}-glucosidase: Major clinical benefits in infantile-onset Pompe disease. *Neurology* 2007;**68**:99–109.

3 Harmatz P, Kramer WG, Hopwood JJ, Simon J, Butensky E, Swiedler SJ, *et al.* Pharmacokinetic profile of recombinant human N-acetylgalactosamine 4-sulphatase enzyme replacement therapy in patients with mucopolysaccharidosis VI (Maroteaux-Lamy syndrome): a phase I/II study 2005;**94**:61–8.

4 Eng CM, Guffon N, Wilcox WR, Germain DP, Lee P, Waldek S, *et al.* Safety and efficacy of recombinant human a -galactosidase A replacement therapy in Fabry's disease. *N Engl J Med* 2001;**345**:9–16.

5 Weinreb NJ, Charrow J, Andersson HC, Kaplan P, Kolodny EH, Mistry P, *et al.* Effectiveness of enzyme replacement therapy in 1028 patients with type 1 Gaucher disease after 2 to 5 years of treatment: a report from the Gaucher Registry. *Am J Med* 2002;**113**:112–9.

6 Schulz A, Ajayi T, Specchio N, de Los Reyes E, Gissen P, Ballon D, *et al.* Study of Intraventricular Cerliponase Alfa for CLN2 Disease. *N Engl J Med* 2018;**378**:1898–907. https://doi.org/10.1056/nejmoa1712649.

7 Cadaoas J, Boyle G, Jungles S, Cullen S, Vellard M, Grubb JH, *et al.* Vestronidase alfa: Recombinant human β-glucuronidase as an enzyme replacement therapy for MPS VII. *Mol Genet Metab* 2020;**130**:65–76. https://doi.org/10.1016/j.ymgme.2020.02.009.

8 Hickman S, Shapiro LJ, Neufeld EF. A recognition marker required for uptake of a lysosomal enzyme by cultured fibroblasts. *Biochem Biophys Res Commun* 1974;**57**:55–61.

9 Zhao KW, Neufeld EF. Purification and characterization of recombinant human alpha-N-acetylglucosaminidase secreted by Chinese hamster ovary cells. *Protein Expr Purif* 2000;**19**:202–11. https://doi.org/10.1006/prep.2000.1230.

10 Weber B, Hopwood JJ, Yogalingam G. Expression and characterization of human recombinant and alpha-N-acetylglucosaminidase. *Protein Expr Purif* 2001;**21**:251–9. https://doi.org/10.1006/prep.2000.1361.

11 Kan S-H, Troitskaya LA, Sinow CS, Haitz K, Todd AK, Di Stefano A, *et al.* Insulin-like growth factor II peptide fusion enables uptake and lysosomal delivery of α-N-acetylglucosaminidase to mucopolysaccharidosis type IIIB fibroblasts. *Biochem J* 2014;**458**:281–9. https://doi.org/10.1042/BJ20130845.

12 Kan S-H, Aoyagi-Scharber M, Le SQSQ, Vincelette J, Ohmi K, Bullens S, *et al.* Delivery of an enzyme-IGFII fusion protein to the mouse brain is therapeutic for mucopolysaccharidosis type IIIB. *Proc Natl Acad Sci* 2014;**111**:14870–5. https://doi.org/10.1073/pnas.1416660111.

bioRxiv preprint doi: https://doi.org/10.1101/2021.08.06.455469; this version posted August 8, 2021. The copyright holder for this preprint (which was not certified by peer review) is the author/funder. All rights reserved. No reuse allowed without permission.

13 Kan S-h, Elsharkawi I, Le SQ, Prill H, Mangini L, Cooper JD, *et al.* Biochemical evaluation of intracerebroventricular rhNAGLU-IGF2 enzyme replacement therapy in neonatal mice with Sanfilippo B syndrome. *Mol Genet Metab* 2021;**133**:185–92. https://doi.org/10.1016/j.ymgme.2021.03.013.

14 *BioMarin Presents Interim Data of Phase 1/2 Study of BMN 250 for Treatment of Sanfilippo B Syndrome (MPS IIIB) at WORLDSymposium™ 2018*. 2018. URL: https://www.prnewswire.com/news-releases/biomarin-presents-interim-data-of-phase-12-study-of-bmn-250-for-treatment-of-sanfilippo-b-syndrome-mps-iiib-at-worldsymposium-2018-300594877.html (Accessed 19 February 2019).

15 *Enzyme replacement therapy, BMN-250, shows promise as treatment for Sanfilippo type B, study finds*. Sanfilippo News. 2019. URL: https://sanfilipponews.com/2019/02/14/bmn-250-shows-promise-treatment-sanfilippo-type-b/.

16 Aoyagi-Scharber M, Crippen-Harmon D, Lawrence R, Vincelette J, Yogalingam G, Prill H, *et al.* Clearance of Heparan Sulfate and Attenuation of CNS Pathology by Intracerebroventricular BMN 250 in Sanfilippo Type B Mice. *Mol Ther - Methods Clin Dev* 2017;**6**:43–53. https://doi.org/10.1016/j.omtm.2017.05.009.

17 Héron B, Mikaeloff Y, Froissart R, Caridade G, Maire I, Caillaud C, *et al.* Incidence and natural history of mucopolysaccharidosis type III in France and comparison with United Kingdom and Greece. *Am J Med Genet A* 2011;**155A**:58–68. https://doi.org/10.1002/ajmg.a.33779.

18 Valstar M, Ruijter G, van Diggelen O, Poorthuis B, Wijburg F. Sanfilippo syndrome: A mini-review. *J Inherit Metab Dis* 2008;**31**:240–52.

19 Belichenko PV V, Dickson PII, Passage M, Jungles S, Mobley WCC, Kakkis EDD. Penetration, diffusion, and uptake of recombinant human á-L-iduronidase after intraventricular injection into the rat brain. *Mol Genet Metab* 2005;**86**:141–9. https://doi.org/10.1016/j.ymgme.2005.04.013.

20 Dickson P, McEntee M, Vogler C, Le S, Levy B, Peinovich M, *et al.* Intrathecal enzyme replacement therapy: successful treatment of brain disease via the cerebrospinal fluid. *Mol Genet Metab* 2007;**91**:61–8. https://doi.org/10.1016/j.ymgme.2006.12.012.

21 Chen A, Vogler C, McEntee MF, Hanson S, Matthew Ellinwood N, Jens J, *et al.* Glycosaminoglycan storage in neuroanatomical regions of mucopolysaccharidosis I dogs following intrathecal recombinant human iduronidase. *APMIS* 2011;**119**:513–21. https://doi.org/10.1111/j.1600-0463.2011.02760.x.

22 Vite CH, Nestrasil I, Mlikotic A, Jens JK, Snella EM, Gross W, *et al.* Features of brain MRI in dogs with treated and untreated mucopolysaccharidosis type I. *Comp Med* 2013;**63**:163–73.

23 Kan S, Le SQ, Bui QD, Benedict B, Cushman J, Sands MS, *et al.* Behavioral deficits and cholinergic pathway abnormalities in male Sanfilippo B mice. *Behav Brain Res* 2016;**312**:265–71. https://doi.org/10.1016/j.bbr.2016.06.023.

24 Heldermon CD, Hennig AK, Ohlemiller KK, Ogilvie JM, Herzog ED, Breidenbach A, *et*

bioRxiv preprint doi: https://doi.org/10.1101/2021.08.06.455469; this version posted August 8, 2021. The copyright holder for this preprint (which was not certified by peer review) is the author/funder. All rights reserved. No reuse allowed without permission.

al. Development of sensory, motor and behavioral deficits in the murine model of Sanfilippo syndrome type B. *PLoS One* 2007;**2**:e772. https://doi.org/10.1371/journal.pone.0000772.

25 Dearborn JT, Harmon SK, Fowler SC, O'Malley KL, Taylor GT, Sands MS, *et al.* Comprehensive functional characterization of murine infantile Batten disease including Parkinson-like behavior and dopaminergic markers. *Sci Rep* 2015;**5**:12752. https://doi.org/10.1038/srep12752.

26 Marsh J, Fensom AH. 4-methylumbelliferyl α-N-acetylglucosaminidase activity for diagnosis of Sanfilippo B disease. *Clin Genet* 2008;**27**:258–62. https://doi.org/10.1111/j.1399-0004.1985.tb00217.x.

27 Lawrence R, Brown JR, Al-Mafraji K, Lamanna WC, Beitel JR, Boons GJ, *et al.* Disease-specific non-reducing end carbohydrate biomarkers for mucopolysaccharidoses. *Nat Chem Biol* 2012;**8**:197–204.

28 Nelvagal HR, Dearborn JT, Ostergaard JR, Sands MS, Cooper JD. Spinal manifestations of CLN1 disease start during the early postnatal period. *Neuropathol Appl Neurobiol* 2020:nan.12658. https://doi.org/10.1111/nan.12658.

29 Egeland MT, Tarczyluk-Wells MM, Asmar MM, Adintori EG, Lawrence R, Snella EM, *et al.* Central nervous system pathology in preclinical MPS IIIB dogs reveals progressive changes in clinically relevant brain regions. *Sci Rep* 2020;**10**:20365. https://doi.org/10.1038/s41598-020-77032-y.

30 Smyth GK, Thorne N, Wettenhall J. *Limma: Linear Models for Microarray Data User's Guide*. 2003. http://www.bioconductor.org.

31 Raudvere U, Kolberg L, Kuzmin I, Arak T, Adler P, Peterson H, *et al.* G:Profiler: A web server for functional enrichment analysis and conversions of gene lists (2019 update). *Nucleic Acids Res* 2019;**47**:W191–8. https://doi.org/10.1093/nar/gkz369.

32 Mumford RA, Mahon LV, Jones S, Bigger B, Canal M, Hare DJ. Actigraphic investigation of circadian rhythm functioning and activity levels in children with mucopolysaccharidosis type III (Sanfilippo syndrome). *J Neurodev Disord* 2015;**7**:31. https://doi.org/10.1186/s11689-015-9126-5.

33 Yogalingam G, Luu AR, Prill H, Lo MJ, Yip B, Holtzinger J, *et al.* BMN 250, a fusion of lysosomal alpha-N-acetylglucosaminidase with IGF2, exhibits different patterns of cellular uptake into critical cell types of Sanfilippo syndrome B disease pathogenesis. *PLoS One* 2019;**14**:e0207836. https://doi.org/10.1371/journal.pone.0207836.

34 Prill H, Luu A, Yip B, Holtzinger J, Lo MJ, Christianson TM, *et al.* Differential Uptake of NAGLU-IGF2 and Unmodified NAGLU in Cellular Models of Sanfilippo Syndrome Type B. *Mol Ther - Methods Clin Dev* 2019;**14**:56–63. https://doi.org/10.1016/j.omtm.2019.05.008.

35 Sands MS, Vogler CA, Ohlemiller KK, Roberts MS, Grubb JH, Levy B, *et al.* Biodistribution, Kinetics, and Efficacy of Highly Phosphorylated and Non-phosphorylated β-Glucuronidase in the Murine Model of Mucopolysaccharidosis VII. *J Biol Chem*

bioRxiv preprint doi: https://doi.org/10.1101/2021.08.06.455469; this version posted August 8, 2021. The copyright holder for this preprint (which was not certified by peer review) is the author/funder. All rights reserved. No reuse allowed without permission.

2001;**276**:43160–5.

36 Le SQ, Kan S-H, Clarke D, Sanghez V, Egeland M, Vondrak KN, *et al.* A Humoral Immune Response Alters the Distribution of Enzyme Replacement Therapy in Murine Mucopolysaccharidosis Type I. *Mol Ther - Methods Clin Dev* 2018;**8**:42–51. https://doi.org/10.1016/j.omtm.2017.09.008.

37 Yu WH, Zhao KW, Ryazantsev S, Rozengurt N, Neufeld EF. Short-term enzyme replacement in the murine model of sanfilippo syndrome type B. *Mol Genet Metab* 2000;**71**:573–80. https://doi.org/10.1006/mgme.2000.3095.

38 Ohmi K, Greenberg DS, Rajavel KS, Ryazantsev S, Li HH, Neufeld EF. Activated microglia in cortex of mouse models of mucopolysaccharidoses I and IIIB. *Proc Natl Acad Sci U S A* 2003;**100**:1902–7.

39 Ausseil J, Desmaris N, Bigou S, Attali R, Corbineau S, Vitry S, *et al.* Early neurodegeneration progresses independently of microglial activation by heparan sulfate in the brain of mucopolysaccharidosis IIIB mice. *PLoS One* 2008;**3**:e2296.

40 DiRosario J, Divers E, Wang C, Etter J, Charrier A, Jukkola P, *et al.* Innate and adaptive immune activation in the brain of MPS IIIB mouse model. *J Neurosci Res* 2009;**87**:978–90. https://doi.org/10.1002/jnr.21912.

41 Fu H, Meadows AS, Ware T, Mohney RP, McCarty DM. Near-Complete Correction of Profound Metabolomic Impairments Corresponding to Functional Benefit in MPS IIIB Mice after IV rAAV9-hNAGLU Gene Delivery. *Mol Ther* 2017;**25**:792–802. https://doi.org/10.1016/j.ymthe.2016.12.025.

42 Fu H, Kang L, Jennings JS, Moy SS, Perez A, DiRosario J, *et al.* Significantly increased lifespan and improved behavioral performances by rAAV gene delivery in adult mucopolysaccharidosis IIIB mice. *Gene Ther* 2007;**14**:1065–77. https://doi.org/10.1038/sj.gt.3302961.

43 Fu H, Samulski RJ, McCown TJ, Picornell YJ, Fletcher D, Muenzer J. Neurological correction of lysosomal storage in a mucopolysaccharidosis IIIB mouse model by adeno-associated virus-mediated gene delivery. *Mol Ther* 2002;**5**:42–9.

44 Kakkis ED, Matynia A, Jonas AJ, Neufeld EF. Overexpression of the human lysosomal enzyme α-L-iduronidase in Chinese hamster ovary cells. *Prot Expr Purif* 1994;**5**:225–32.

45 Clarke D, Pearse Y, Kan S-h, Le SQ, Sanghez V, Cooper JD, *et al.* Genetically Corrected iPSC-Derived Neural Stem Cell Grafts Deliver Enzyme Replacement to Affect CNS Disease in Sanfilippo B Mice. *Mol Ther - Methods Clin Dev* 2018;**10**:113–27. https://doi.org/10.1016/j.omtm.2018.06.005.

46 Lin HY, Chen MR, Lin SM, Hung CL, Niu DM, Chang TM, *et al.* Cardiac characteristics and natural progression in Taiwanese patients with mucopolysaccharidosis III. *Orphanet J Rare Dis* 2019;**14**:140. https://doi.org/10.1186/s13023-019-1112-7.

47 Nijmeijer SCM, de Bruin-Bon RHACM, Wijburg FA, Kuipers IM. Cardiac disease in mucopolysaccharidosis type III. *J Inherit Metab Dis* 2019;**42**:276–85. https://doi.org/10.1002/jimd.12015.

bioRxiv preprint doi: https://doi.org/10.1101/2021.08.06.455469; this version posted August 8, 2021. The copyright holder for this preprint (which was not certified by peer review) is the author/funder. All rights reserved. No reuse allowed without permission.

48 Chiravuri M, Agarraberes F, Mathieu SL, Lee H, Huber BT. Vesicular Localization and Characterization of a Novel Post-Proline-Cleaving Aminodipeptidase, Quiescent Cell Proline Dipeptidase. *J Immunol* 2000;**165**:5695–702. https://doi.org/10.4049/jimmunol.165.10.5695.

49 Sadir R, Imberty A, Baleux F, Lortat-Jacob H. Heparan sulfate/heparin oligosaccharides protect stromal cell-derived factor-1 (SDF-1)/CXCL12 against proteolysis induced by CD26/dipeptidyl peptidase IV. *J Biol Chem* 2004;**279**:43854–60. https://doi.org/10.1074/jbc.M405392200.